

The use of early data on $B \rightarrow \rho\pi$ decays

Helen R. Quinn and João P. Silva*

Stanford Linear Accelerator Center, Stanford University, Stanford, CA 94309, USA

(October 25, 2018)

This paper reviews the Dalitz plot analysis for the decays $B^0(\bar{B}^0) \rightarrow \rho\pi \rightarrow \pi^+\pi^-\pi^0$. We discuss what can be learned about the ten parameters in this analysis from untagged and from tagged time-integrated data. We find that, with the important exception of the interesting CP violating quantity α , the parameters can be determined from this data sample – and, hence, they can be measured at CLEO as well as at the asymmetric B factories. This suggests that the extraction of α from the time-dependent data sample can be accomplished with a smaller data sample (and, therefore, sooner) than would be required if all ten parameters were to be obtained from that time-dependent data sample alone. We also explore bounds on the shift of the true angle α from the angle measured from charged ρ final states alone. These may be obtained prior to measurements of the parameters describing the neutral ρ channel, which are expected to be small.

11.30.Er, 13.25.Hw, 14.40.-n.

I. INTRODUCTION

The B factories at SLAC and KEK are now collecting data and expect to produce measurements of the CP asymmetry in the mode $B \rightarrow J/\psi K_S$ within one year, measuring $\sin 2\beta$. Preliminary results on this mode from CDF [1] already indicate that it is unlikely that a discrepancy with the Standard Model will be found from this result alone. This means that tests of the Standard Model mechanism for CP violation will rely upon our ability to measure further CP -violating parameters, such as the angle $\alpha = \pi - \beta - \gamma$ of the Unitarity triangle, with sufficient accuracy to be sensitive to Standard Model relationships. This will require that we master the removal of theoretical uncertainties due to penguin diagrams in at least one of the available channels. So far there are two sets of candidate decay modes, $\pi\pi$ [2] and $\rho\pi$ [3], for which analyses to extract α using isospin relationships have been suggested. The first suffers from relatively small branching ratios [4] and from the experimental difficulty of measuring the $\pi^0\pi^0$ branching ratio. Some of the modes for the second case have recently been observed at CLEO [5]. These results are encouraging. They are close to model-dependent predictions and, hence, appear to reinforce estimates that the analysis suggested by Snyder and Quinn will require of order 180 fb^{-1} , or six years of running at BABAR design luminosity, to complete [6].

This paper revisits that analysis and reviews what intermediate steps can be made with earlier data samples. In particular we stress that many of the parameters relevant to the extraction of α can be predetermined from untagged, and from tagged but time-integrated data samples. The benefit of this is that, once this is done, only the CP -violating parameter α remains to be fit to the full tagged and time-dependent Dalitz plot. Presumably it will then be possible to perform the $\rho\pi$ analysis with smaller data samples than those needed if the full set of ten parameters is fit to the tagged, time-dependent sample alone (as has been done to date in Monte Carlo studies of this mode). We also discuss bounds on the shift in α from penguin contributions. These can be obtained, by methods similar to those previously suggested for the $\pi\pi$ modes [7–9], even if the $\rho^0\pi^0$ amplitude is too small to be measured directly. We will also discuss a bound which applies only in the $\rho\pi$ case, having no parallel in the $\pi\pi$ case.

This paper presents a purely theoretical discussion, with no simulations and no attempt to address issues of backgrounds or of other modes that may contribute to the $\pi^+\pi^-\pi^0$ Dalitz plot [10]. Certainly these issues will be important. The larger untagged data sample will also be the first place to explore the issues of further contributions to the Dalitz plot. The approach of fixing as many parameters as possible from the untagged and from the tagged but time-integrated data samples, combined with improvements in machine luminosity, such as those already under study for PEP-II, may make the extraction of a reliable value for α a reality on a somewhat faster time scale than suggested by the estimates based on fits to tagged data only.

*Permanent address: Instituto Superior de Engenharia de Lisboa, Rua Conselheiro Emídio Navarro, 1900 Lisboa, Portugal.

II. NOTATION

A. Isospin decomposition

We are interested in the decays from B^+ and B^0 into $\rho\pi$ final states. The decay amplitudes can be classified according to isospin: $\{B^+, B^0\}$ form an isospin doublet; the final state $\rho\pi$ can have isospin $I_f = 0$, $I_f = 1$, and $I_f = 2$ components. In general, the final state with $I_f = 0$ can only be reached with operators having $\Delta I = 1/2$; the final state with $I_f = 1$ can be reached with operators having $\Delta I = 1/2$ or $\Delta I = 3/2$; and the final state with $I_f = 2$ can be reached with operators having $\Delta I = 3/2$ or $\Delta I = 5/2$. We denote the isospin amplitudes by $A_{\Delta I, I_f}$. Thus,

$$\begin{aligned}
a_{+0} &= a(B^+ \rightarrow \rho^+ \pi^0) = \frac{1}{2} \sqrt{\frac{3}{2}} A_{3/2,2} - \frac{1}{2} \frac{1}{\sqrt{2}} A_{3/2,1} + \frac{1}{\sqrt{2}} A_{1/2,1} \left[-\frac{1}{\sqrt{6}} A_{5/2,2} \right], \\
a_{0+} &= a(B^+ \rightarrow \rho^0 \pi^+) = \frac{1}{2} \sqrt{\frac{3}{2}} A_{3/2,2} + \frac{1}{2} \frac{1}{\sqrt{2}} A_{3/2,1} - \frac{1}{\sqrt{2}} A_{1/2,1} \left[-\frac{1}{\sqrt{6}} A_{5/2,2} \right], \\
a_{+-} &= a(B^0 \rightarrow \rho^+ \pi^-) = \frac{1}{2\sqrt{3}} A_{3/2,2} + \frac{1}{2} A_{3/2,1} + \frac{1}{2} A_{1/2,1} + \frac{1}{\sqrt{6}} A_{1/2,0} \left[+\frac{1}{2\sqrt{3}} A_{5/2,2} \right], \\
a_{-+} &= a(B^0 \rightarrow \rho^- \pi^+) = \frac{1}{2\sqrt{3}} A_{3/2,2} - \frac{1}{2} A_{3/2,1} - \frac{1}{2} A_{1/2,1} + \frac{1}{\sqrt{6}} A_{1/2,0} \left[+\frac{1}{2\sqrt{3}} A_{5/2,2} \right], \\
a_{00} &= a(B^0 \rightarrow \rho^0 \pi^0) = \frac{1}{\sqrt{3}} A_{3/2,2} - \frac{1}{\sqrt{6}} A_{1/2,0} \left[+\frac{1}{\sqrt{3}} A_{5/2,2} \right].
\end{aligned} \tag{1}$$

Similar relations hold for the \bar{B}^0 decay amplitudes, which we denote by \bar{a}_{-0} , \bar{a}_{0-} , \bar{a}_{-+} , \bar{a}_{+-} , and \bar{a}_{00} , respectively. Note that our notation here is that \bar{a}_{ij} is the amplitude for the \bar{B}^0 to decay to a ρ of charge i and a π of charge j . The CP relationships are thus $CP(a_{ij}) = \bar{a}_{-i, -j}$. The \bar{B}^0 isospin components are $\bar{A}_{\Delta I, I_f}$.

In the Standard Model, there are tree-level amplitudes, gluonic penguin amplitudes, electroweak penguin amplitudes, and final state rescattering effects. The tree level $b \rightarrow u\bar{u}d$ decays have both $\Delta I = 1/2$ and $\Delta I = 3/2$ components. In contrast, the gluonic $b \rightarrow d$ penguins are pure $\Delta I = 1/2$, because the gluon is pure $I = 0$. Therefore, the isospin amplitudes $A_{3/2,1}$ and $A_{3/2,2}$ only receive contributions (and, thus, weak phases) from the tree-level diagrams. There are no diagrammatic $\Delta I = 5/2$ contributions at this order; such effects arise only from electromagnetic corrections to the weak-decay diagrams.

A priori, there is no hierarchy among the $\Delta I = 1/2$ and $\Delta I = 3/2$ isospin amplitudes. However, the combination of isospin amplitudes involved in the decay $B^0 \rightarrow \rho^0 \pi^0$ is generally argued to be suppressed because the tree-level and gluonic penguin diagrams can only contribute to $B^0 \rightarrow \rho^0 \pi^0$ through a color-suppressed recombination of the quarks in the final state. This argument is not theoretically rigorous because $B^0 \rightarrow \rho^0 \pi^0$ may be fed from other topologies through strong final state rescattering. Eventually experiment will tell us whether these effects are important.

In what follows we will neglect two contributions which are suppressed in the SM. The first contribution arises from the electroweak penguin diagrams, which have the same weak phase structure as the QCD penguin diagrams, but contribute to both $\Delta I = 1/2$ and $\Delta I = 3/2$ amplitudes. As a result, the electroweak penguin contributions are not removed by the isospin-based analyses. However, they are expected to be very small in these channels [6,11]. The second contribution is due to a possible $\Delta I = 5/2$ isospin component, included within square brackets in Eqs. (1). In the SM, this component comes from electromagnetic rescattering effects and, thus, it is suppressed by $\alpha \sim 1/127$.¹ Both effects could become relevant for $B^0 \rightarrow \rho^0 \pi^0$, should this amplitude turn out to be very small.

Henceforth, we will only consider the tree-level and gluonic penguin diagrams. These give contributions with weak phases

$$\begin{aligned}
\frac{V_{ub}^* V_{ud}}{|V_{ub}^* V_{ud}|} &= e^{i\gamma} = -e^{-i(\beta+\alpha)}, \\
\frac{V_{tb}^* V_{td}}{|V_{tb}^* V_{td}|} &= e^{-i\beta}.
\end{aligned} \tag{2}$$

¹Notice, however, that this effect is important in $K \rightarrow \pi\pi$ decays because there one has a strong hierarchy among the decay amplitudes, $\text{Re}A_2/\text{Re}A_0 \sim 1/22$, encoded into the $\Delta I = 1/2$ rule [13–15].

The first of these expressions is the weak phase of the tree-level contributions. Here we follow [12] and use the unitarity relationship to rewrite the penguin contribution as a dominant term proportional to the second of the CKM factors in Eq. (2) plus a sub-dominant term proportional to the first CKM factor in Eq. (2).² In what follows we always subsume this second term within the amplitudes we refer to as $\Delta I = 1/2$ tree amplitudes. Since we do not calculate these quantities, but rather discuss extracting them from fits to experiment, this makes no difference to our analysis. Note, however, that if the amplitudes extracted in this way are to be compared to those calculated in any given model, then the penguin contributions to our so-called “tree” amplitudes must be taken into account.

The interference between the two amplitude contributions in Eq. (2) depends on the weak phase α . However, we will show that, as is usual with direct CP -violation effects, any sensitivity to α is masked by an unknown coefficient with large theoretical uncertainty. Another weak phase arises from the interference between the $B^0 - \overline{B}^0$ mixing, $q/p = \exp[-2i(\beta - \theta_d)]$, and the tree-level diagrams. For example,

$$\frac{q}{p} \frac{\overline{A}_{3/2,2}}{A_{3/2,2}} = e^{-2i(\beta - \theta_d)} e^{-2i\gamma} = e^{2i(\alpha + \theta_d)}, \quad (3)$$

where θ_d parametrizes a possible new physics contribution to the phase in $B^0 - \overline{B}^0$ mixing. In the SM, $\theta_d = 0$ and the two phases coincide; other models have $\theta_d \neq 0$ and a difference arises. The phase probed by the Snyder–Quinn method is $\alpha + \theta_d$ [14].

B. $B^0 \rightarrow \pi^+ \pi^- \pi^0$ decay amplitudes

The ρ -mediated $B^0 \rightarrow \pi^+ \pi^- \pi^0$ decay amplitudes may be written as

$$\begin{aligned} A &= a(B^0 \rightarrow \pi^+ \pi^- \pi^0) = f_+ a_{+-} + f_- a_{-+} + f_0 a_{00}, \\ \overline{A} &= a(\overline{B}^0 \rightarrow \pi^+ \pi^- \pi^0) = f_+ \overline{a}_{+-} + f_- \overline{a}_{-+} + f_0 \overline{a}_{00}, \end{aligned} \quad (4)$$

where f_{\pm} and f_0 are Breit-Wigner functions representing ρ^{\pm} and ρ^0 , respectively, and also include the $\cos\theta$ angular dependences of the helicity zero ρ decays. The crucial observation made by Snyder and Quinn is that the Breit-Wigner functions contain CP -even phases, and that the interference between the different Breit-Wigner shapes across the Dalitz plot provides experimental sensitivity to the weak and strong phases contained in Eqs. (4). There is some systematic uncertainty associated with the specific choice made for the shape of the functions f_{\pm} and f_0 . This uncertainty affects primarily the corners of the Dalitz plot where the tails of two such functions interfere; these are the regions of the Dalitz plot from which one extracts the interference between two distinct decay amplitudes.

It will prove convenient to rewrite Eqs. (4) as

$$\begin{aligned} A &= f_c a_c + f_d a_d + f_n a_n, \\ \overline{A} &= f_c \overline{a}_c + f_d \overline{a}_d + f_n \overline{a}_n, \end{aligned} \quad (5)$$

where

$$f_c = \frac{f_+ + f_-}{2}, \quad f_d = \frac{f_+ - f_-}{2}, \quad f_n = \frac{f_0}{2}, \quad (6)$$

and

$$\begin{aligned} a_c &= a_{+-} + a_{-+}, & a_d &= a_{+-} - a_{-+}, & a_n &= 2a_{00}, \\ \overline{a}_c &= \overline{a}_{+-} + \overline{a}_{-+}, & \overline{a}_d &= \overline{a}_{+-} - \overline{a}_{-+}, & \overline{a}_n &= 2\overline{a}_{00}. \end{aligned} \quad (7)$$

Notice that the CP -conjugate of a_d is not \overline{a}_d , but rather $-\overline{a}_d$.

As discussed in the appendix, we parametrize the amplitudes a_c , a_d , and a_n as

²The term is sub-dominant in that it is a difference of up and charm quark contributions and, hence, it vanishes in the limit that these two quark masses are taken to be equal.

$$\begin{aligned}
a_c &= T e^{-i\alpha} (1 - z - r_0), \\
a_d &= T e^{-i\alpha} (z_1 + r_1), \\
a_n &= T e^{-i\alpha} (z + r_0),
\end{aligned} \tag{8}$$

where z and z_1 are CP -even, while r_0 and r_1 are CP -odd. The quantity $T z_1$ contains the CP -even contributions to the final state with $I_f = 1$, summing the tree amplitude and the penguin amplitude multiplied by $\cos\alpha$. $T r_1$ ($T r_0$) contains the CP -odd part, given by the penguin contributions to the final state with $I_f = 1$ ($I_f = 0$), multiplied by $i \sin\alpha$. Similarly, the amplitudes contained in $q\bar{A}_f/p$ can be written as

$$\begin{aligned}
\frac{q}{p}\bar{a}_c &= e^{2i\theta_d} T e^{i\alpha} (1 - z + r_0), \\
\frac{q}{p}\bar{a}_d &= e^{2i\theta_d} T e^{i\alpha} (-z_1 + r_1), \\
\frac{q}{p}\bar{a}_n &= e^{2i\theta_d} T e^{i\alpha} (z - r_0).
\end{aligned} \tag{9}$$

We have chosen to define strong phases so that T is a real positive quantity. Notice that $a_c + a_n = T e^{-i\alpha}$, and $q/p(\bar{a}_c + \bar{a}_n) = e^{2i\theta_d} T e^{i\alpha}$. Therefore, the imaginary (real) part of the ratio of these quantities, measures the sine (cosine) of the phase in Eq. (3).

If a_{00} and \bar{a}_{00} are indeed color suppressed, then z and r_0 will be smaller than 1, z_1 and r_1 . In that case, the CP -violating difference

$$\frac{|a_c|^2 - |\bar{a}_c|^2}{2T^2} = -2\text{Re } r_0 + 2\text{Re}(z r_0^*) \tag{10}$$

will also be small.

In connection with Eqs. (4) and (5), there is no advantage of one parametrization with respect to another. We could equally well have chosen to write the amplitudes in a new set of basis functions $\{f_1, f_2, f_3\}$, given by

$$f_1 = \frac{f_+ + f_- + 2f_0}{6}, \quad f_2 = \frac{f_+ - f_-}{2}, \quad f_3 = \frac{f_+ + f_- - f_0}{3}. \tag{11}$$

In this basis, the amplitudes would become

$$\begin{aligned}
A &= f_1 (a_c + a_n) + f_2 a_d + f_3 (a_c - a_n/2) \\
\bar{A} &= f_1 (\bar{a}_c + \bar{a}_n) + f_2 \bar{a}_d + f_3 (\bar{a}_c - \bar{a}_n/2).
\end{aligned} \tag{12}$$

Eqs. (4) highlight the intermediate $\rho\pi$ states; Eqs. (5) highlight the CP structure of the intermediate charged $\rho\pi$ states, but still treat the intermediate $\rho^0\pi^0$ separately; and Eqs. (12) highlight the extraction of $a_c + a_n = T e^{-i\alpha}$. Although each basis has its pedagogical advantages, they have no experimental significance. What one does experimentally is a maximum likelihood fit of the variables T , z_1 , r_1 , z , and r_0 to all the data in the Dalitz plots.

C. Observables in the decay rates

In the B_d system we have $|q/p| \sim 1$ and $\Delta\Gamma \ll \Gamma$. Therefore,

$$\Gamma[B^0 \rightarrow f] + \Gamma[\bar{B}^0 \rightarrow f] \propto |A_f|^2 + |\bar{A}_f|^2, \tag{13}$$

$$\Gamma[B^0 \rightarrow f] - \Gamma[\bar{B}^0 \rightarrow f] \propto (|A_f|^2 - |\bar{A}_f|^2) \cos \Delta m t - 2\text{Im} \left(\frac{q}{p} \bar{A}_f A_f^* \right) \sin \Delta m t. \tag{14}$$

One may rewrite these expressions using $\lambda_f = q\bar{A}_f/(pA_f)$.³ The three terms in Eqs. (13) and (14) become $1 + |\lambda_f|^2$, $1 - |\lambda_f|^2$, and $\text{Im}\lambda_f$, respectively. The untagged decay rate in Eq. (13) probes only the combination $1 + |\lambda_f|^2$, regardless of whether these measurements are time-dependent or time-integrated. Due to the anti-symmetric nature

³Notice, however, that some authors use the opposite sign convention for q/p and, thus, for λ_f .

of the $B^0 - \bar{B}^0$ pairs produced at the $\Upsilon(4s)$, tagged, time-integrated measurements performed at facilities working on this resonance can probe $1 + |\lambda_f|^2$ and $1 - |\lambda_f|^2$, but not $\text{Im}\lambda_f$.

If f is a CP eigenstate and the decay amplitudes A_f and \bar{A}_f are defined in such a way that the rates $|A_f|^2$ and $|\bar{A}_f|^2$ include all the phase space integrations, then $1 + |\lambda_f|^2$ is CP-even, while $1 - |\lambda_f|^2$ and $\text{Im}\lambda_f$ are CP-odd. Under these conditions, the ratio of Eq. (14) to Eq. (13) is the famous CP-violating asymmetry. It is sometimes stated that one can only probe $\text{Im}\lambda_f/(1 + |\lambda_f|^2)$. While this is true if one looks only at the CP-violating asymmetry, one can see from Eqs. (13) and (14) that, in principle, there is enough information in the two decay rates for a clean determination of $\text{Im}\lambda_f$. The caveat is that disentangling $\text{Im}\lambda_f$ from $1 \pm |\lambda_f|^2$ requires that all these quantities be affected by the same normalization. This may not be true once the experimental cuts, in particular possible cuts on the time t , are folded into the analysis.

Using Eqs. (5) we find

$$|A|^2 \pm |\bar{A}|^2 = \sum_i (|a_i|^2 \pm |\bar{a}_i|^2) |f_i|^2 + 2 \sum_{i<j} \text{Re} [f_i f_j^* (a_i a_j^* \pm \bar{a}_i \bar{a}_j^*)], \quad (15)$$

where i and j can take the values c, d , and n . The notation $i < j$ means that the (i, j) pairs are not repeated. Untagged decays probe the observables corresponding to the + sign. Tagged, time-integrated decays probe the observables with both signs (or, what is the same, they measure $|A|^2$ and $|\bar{A}|^2$ separately). Since the functions f_i are quite distinct in their Dalitz plot structure one can treat the coefficient of each different pair $f_i f_j^*$ as a separate observable.⁴ We may define the nine untagged observables by

$$\frac{|A|^2 + |\bar{A}|^2}{2} = T^2 \left[\sum_i U_{ii} |f_i|^2 + 2 \sum_{i<j} U_{ij}^R \text{Re} (f_i f_j^*) - 2 \sum_{i<j} U_{ij}^I \text{Im} (f_i f_j^*) \right], \quad (16)$$

where

$$\begin{aligned} U_{ii} &= \frac{|a_i|^2 + |\bar{a}_i|^2}{2T^2}, \\ U_{ij}^R &= \frac{\text{Re} (a_i a_j^* + \bar{a}_i \bar{a}_j^*)}{2T^2} \quad (i \neq j), \\ U_{ij}^I &= \frac{\text{Im} (a_i a_j^* + \bar{a}_i \bar{a}_j^*)}{2T^2} \quad (i \neq j). \end{aligned} \quad (17)$$

We will refer to these observables generically as the U -observables. We may define similar quantities with U replaced by D to describe the corresponding observables obtained for the difference $|A|^2 - |\bar{A}|^2$. These D -observables are obtained from Eqs. (17) by replacing the '+' signs with '-' signs.

Using Eqs. (8) and (9), the untagged observables are

$$U_{cc} = \frac{|a_c|^2 + |\bar{a}_c|^2}{2T^2} = |1 - z|^2 + |r_0|^2, \quad (18)$$

$$U_{dd} = \frac{|a_d|^2 + |\bar{a}_d|^2}{2T^2} = |z_1|^2 + |r_1|^2, \quad (19)$$

$$U_{cd}^R + iU_{cd}^I = \frac{a_c a_d^* + \bar{a}_c \bar{a}_d^*}{2T^2} = r_1^* - z r_1^* - r_0 z_1^*, \quad (20)$$

$$U_{cn}^R + iU_{cn}^I = \frac{a_c a_n^* + \bar{a}_c \bar{a}_n^*}{2T^2} = z^* - |z|^2 - |r_0|^2, \quad (21)$$

$$U_{dn}^R + iU_{dn}^I = \frac{a_d a_n^* + \bar{a}_d \bar{a}_n^*}{2T^2} = z_1 r_0^* + r_1 z^*, \quad (22)$$

$$U_{nn} = \frac{|a_n|^2 + |\bar{a}_n|^2}{2T^2} = |z|^2 + |r_0|^2. \quad (23)$$

⁴Note, however, that the errors in the extraction of these various observables are correlated. Thus, our observables, while distinct are not technically independent. A discussion of error correlations is beyond the scope of this paper, but will of course be important in the application of this approach to data.

Thus the U_i contain nine different functions of the four complex parameters z_i, r_i . The requirement that the combination $U_{cc} + 2U_{cn}^R + U_{nn}$ equals 1 yields the overall normalization T .

Similarly, the tagged, time-integrated measurements will provide the additional observables

$$D_{cc} = \frac{|a_c|^2 - |\bar{a}_c|^2}{2T^2} = -2\text{Re } r_0 + 2\text{Re}(zr_0^*), \quad (24)$$

$$D_{dd} = \frac{|a_d|^2 - |\bar{a}_d|^2}{2T^2} = 2\text{Re}(z_1 r_1^*), \quad (25)$$

$$D_{cd}^R + iD_{cd}^I = \frac{a_c a_d^* - \bar{a}_c \bar{a}_d^*}{2T^2} = z_1^* - z z_1^* - r_0 r_1^* \quad (26)$$

$$D_{cn}^R + iD_{cn}^I = \frac{a_c a_n^* - \bar{a}_c \bar{a}_n^*}{2T^2} = r_0^* - 2\text{Re}(zr_0^*), \quad (27)$$

$$D_{dn}^R + iD_{dn}^I = \frac{a_d a_n^* - \bar{a}_d \bar{a}_n^*}{2T^2} = z_1 z^* + r_1 r_0^*, \quad (28)$$

$$D_{nn} = \frac{|a_n|^2 - |\bar{a}_n|^2}{2T^2} = 2\text{Re}(zr_0^*). \quad (29)$$

Note that $D_{cc} + 2D_{cn}^R + D_{nn} = 0$; thus only eight different combinations of T, z_1, r_1, z , and r_0 get fixed by measurements of the D -observables.

Much can be learned about the interplay between the Dalitz plot analysis and CP -violation by looking at Eqs. (18) through (29). From the definitions of r_0 and r_1 in Eqs. (A3), we know that these quantities involve the product of a penguin contribution with $\sin \alpha$. Any nonzero value for r_0 and/or r_1 signals direct CP -violation. It is true that such quantities do not by themselves allow us to determine the size of CP -violation, because $\sin \alpha$ appears multiplied by an unknown parameter; the theoretical calculation of this parameter is plagued by large hadronic uncertainties. (This is as expected for any observable probing direct CP -violation.)

As expected, the quantities $D_{cc}, D_{dd}, D_{cn}^R, D_{cn}^I$, and D_{nn} are CP -odd. Surprisingly, the quantities $U_{cd}^R, U_{cd}^I, U_{dn}^R$, and U_{dn}^I are also CP -odd, despite the fact that they are obtained by looking for untagged decays. How does this come about? The reason is that there is a source of sensitivity to CP -violation induced in the Dalitz plot analysis by the fact that ρ_+ and ρ_- are CP -conjugate of each other. Said otherwise, when one performs a CP -transformation on $f_+ a_{+-}$, one obtains $f_- \bar{a}_{-+}$ and not a quantity proportional to f_+ . As pointed out before, this means that a CP transformation on a_d yields $-\bar{a}_d$. Therefore, the quantities linear in a_d and \bar{a}_d have peculiar CP -properties; $U_{cd}^R, U_{cd}^I, U_{dn}^R$, and U_{dn}^I are CP -odd, while $D_{cd}^R, D_{cd}^I, D_{dn}^R$, and D_{dn}^I are CP -even.

Additional observables are obtained in the tagged, time-dependent decays, which contain a $\sin \Delta m t$ term given by

$$\text{Im} \left(\frac{q}{p} \bar{A} A^* \right) = T^2 \left[\sum_i I_{ii} |f_i|^2 + \sum_{i < j} I_{ij}^I \text{Re} (f_i f_j^*) + \sum_{i < j} I_{ij}^R \text{Im} (f_i f_j^*) \right]. \quad (30)$$

Here

$$\begin{aligned} I_{ii} &= \text{Im} \left(\frac{q}{p} \bar{a}_i a_i^* \right) / T^2, \\ I_{ij}^I &= \text{Im} \left[\frac{q}{p} (\bar{a}_i a_j^* + \bar{a}_j a_i^*) \right] / T^2 \quad (i \neq j), \\ I_{ij}^R &= \text{Re} \left[\frac{q}{p} (\bar{a}_i a_j^* - \bar{a}_j a_i^*) \right] / T^2 \quad (i \neq j). \end{aligned} \quad (31)$$

As before, i and j take the values c, d , and n , and the notation $i < j$ means that no (i, j) pair gets repeated in the sum. As a result, we have nine new observables. These observables depend on $\sin 2(\alpha + \theta_d)$ and $\cos 2(\alpha + \theta_d)$, with coefficients given in table I.

We stress that the uncertainties associated with the exact shape chosen for the ρ resonances are likely to affect the U_{ii}, D_{ii} , and I_{ii} coefficients less than they affect the coefficients U_{ij}, D_{ij} , and I_{ij} with $i \neq j$.

III. ANALYSIS

This section reviews what can be learned in the various experimental searches. Eight of the ten parameters needed to extract α can be fit with untagged decays alone. This greatly increases the data sample that will be available for

determining these parameters, since at the B -factories tagging efficiencies are estimated to be of order 0.3 (or less). Further, many questions about backgrounds and the contributions of the other resonances to the three pion Dalitz plot can also begin to be answered using this larger data sample of untagged events; though they must also be re-examined in the tagged data sample, where non- B background will presumably be reduced. Fitting to tagged, time-integrated events, fixes one further parameter and gives eight additional measurements that depend on combinations of the eight parameters already fixed, thus improving the precision of their determination. Only the important CP -violating CKM-related parameter $\alpha + \theta_d$ remains to be fit to the tagged time-dependent Dalitz plot data. Our conclusion is that these preliminary steps can and should be performed at both symmetric and asymmetric B -factories.

A. Observables from untagged decays

The observables U_{cc} through U_{nn} can be combined to yield T , z , r_1 , $|z_1|$, $|r_0|$ and $\arg(z_1 r_0^*)$. Therefore, the nine observables present in untagged decays, U_{cc} through U_{nn} , allow us to measure eight quantities and give one mathematically redundant piece of information, which of course serves to further constrain that combination of observables.

The result of this analysis is that the large data sample of untagged decays is extremely important for the final determination of α in the $B \rightarrow \rho\pi$ channels. One may use untagged decays to measure all relevant quantities except one angle—the angle between z_1 (or r_0) and z (or r_1)—and the CP -violating phase $\alpha + \theta_d$. Moreover, one will be sensitive to direct CP -violation through $|r_0|$ and $|r_1|$.

B. Observables from tagged time-integrated decays

The subset of events corresponding to tagged, time-integrated decays will provide measurements of the additional observables D_{cc} through D_{nn} . Since U_{nn} and D_{nn} are expected to be small, it is interesting to note that the remaining 16 U - and D -observables are sufficient to fix the nine parameters T , z_1 , r_1 , z , and r_0 , and give seven mathematically redundant pieces of information. That means that one does not need to probe quantities quadratic in $|a_n|$ and $|\bar{a}_n|$ (that is, one does not need to have an observable $\rho^0\pi^0$ branching fraction) in order to determine all the observables attainable with these measurements. Should U_{nn} and D_{nn} be measured, they will provide two further mathematically redundant pieces of information. All these nine parameters have model-independent information that, like a branching fraction, can be taken from one experiment and used as input in another. Therefore, these experiments can and should be performed both at CLEO and at the asymmetric B -factories. The advantage of this is that fewer parameters remain to be determined from the relatively small time-dependent data sample.

C. Observables from tagged time-dependent decays

Once a data sample of tagged, time-dependent events is available, their rates contain a $\sin \Delta m t$ term, allowing for a measurement of I_{cc} through I_{nn} . (One expects that, for some time to come, this data sample will be small compared to the data samples discussed above.) The I -observables depend on $\sin 2(\alpha + \theta_d)$ and $\cos 2(\alpha + \theta_d)$, with coefficients given in table I. We have already seen that the combination of untagged and tagged time-independent decays yield T , z_1 , r_1 , z , and r_0 . These must now be combined with the observables in I_{cc} through I_{nn} . A combination of any pair of these I -observables yields $\sin 2(\alpha + \theta_d)$ and $\cos 2(\alpha + \theta_d)$ independently. A fit to all the observables determines $2(\alpha + \theta_d)$ (up to discrete ambiguities) and provides additional mathematically redundant pieces of information.

We should point out that, as expected, one cannot extract $\alpha + \theta_d$ unless some information is known about quantities linear in a_n and \bar{a}_n . However, since these amplitudes into neutral $\rho^0\pi^0$ might be color suppressed, it is interesting to ask what one may learn while only bounds, rather than measurements, on $|a_n|$ and $|\bar{a}_n|$ are known. In section IV we will show that *bounds* on these quantities can be combined with *measurements* of quantities involving the charged $\rho^\pm\pi^\mp$ channels in order to determine $\alpha + \theta_d$, up to an error that decreases with $|a_n|$ and $|\bar{a}_n|$.

IV. TWO USEFUL BOUNDS

In this section we suppose that the bands in the Dalitz plot corresponding to $B \rightarrow \rho^\pm\pi^\mp$ have been measured while only bounds on the pieces linear and quadratic in a_n and \bar{a}_n are known. We will show that one may still find bounds on $\alpha + \theta_d$, with an error that decreases as $|a_n|$ and $|\bar{a}_n|$ decrease.

A. One useful bound

As we have seen before, a measurement of quantities which are independent of a_n and \bar{a}_n is not enough for a determination of $\alpha + \theta_d$. In particular, we can see from Eqs. (18), (24) and the first entry in Table 1 that measuring the parameters U_{cc} , D_{cc} , and I_{cc} , which refer only to the decays into $\rho^\pm \pi^\mp$, is enough to determine⁵

$$\frac{I_{cc}}{\sqrt{U_{cc}^2 - D_{cc}^2}} = \frac{\text{Im}\left(\frac{q}{p} \frac{\bar{a}_c}{a_c}\right)}{\left|\frac{q}{p} \frac{\bar{a}_c}{a_c}\right|} = \sin[2(\alpha + \theta_d + \delta_\alpha)], \quad (32)$$

where we have defined

$$2\delta_\alpha = \arg\left(\frac{1-z+r_0}{1-z-r_0}\right). \quad (33)$$

Unfortunately, δ_α is neither zero nor calculable.

However, as we will now show, bounds on $|a_n|$ and $|\bar{a}_n|$ are enough to constrain δ_α . As these bounds decrease, the deviation of Eq. (32) from $\sin 2(\alpha + \theta_d)$ also decreases.

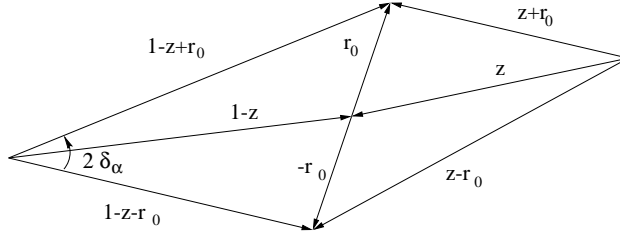


FIG. 1. Triangle construction for $1-z \pm r_0$ and $z \pm r_0$. These complex numbers are related to \bar{a}_c , a_c , a_n , and \bar{a}_n , respectively.

To prove this, we use Fig. 1 to derive

$$|2r_0|^2 = |1-z+r_0|^2 + |1-z-r_0|^2 - 2|1-z+r_0||1-z-r_0| \cos(2\delta_\alpha), \quad (34)$$

and

$$|2r_0| \leq |z+r_0| + |z-r_0|. \quad (35)$$

Using these equations and the expressions for $|a_n|$, $|\bar{a}_n|$, $|a_c|$, and $|\bar{a}_c|$ in Eqs. (8) and (9), we find

$$\sin^2 \delta_\alpha \leq \frac{(|a_n| + |\bar{a}_n|)^2 - (|a_c| - |\bar{a}_c|)^2}{4|a_c \bar{a}_c|}. \quad (36)$$

Notice that, since we assume $|a_c|$ and $|\bar{a}_c|$ to be known, we only need to know bounds on quantities linear in a_n and \bar{a}_n in order to get bounds on $|a_n|$ and $|\bar{a}_n|$. The observables quadratic in a_n and \bar{a}_n are not needed. We have thus proved that one can determine $(\alpha + \theta_d)$ by *measuring* only quantities from charged $\rho^\pm \pi^\mp$ final states, up to an error that decreases as the *bounds* on the color suppressed amplitudes $B \rightarrow \rho^0 \pi^0$ decrease.

It is interesting to compare the bound in Eq. (36), with similar bounds obtained previously for the $B \rightarrow \pi\pi$ decays [7–9]. We note a similarity between the parametrization of the $B \rightarrow \pi\pi$ decays and the parametrization of the $B \rightarrow \rho\pi$ decays, related through

$$\begin{aligned} a_n &\leftrightarrow 2A(B^0 \rightarrow \pi^0 \pi^0), \\ a_c &\leftrightarrow \sqrt{2}A(B^0 \rightarrow \pi^+ \pi^-), \end{aligned} \quad (37)$$

⁵Notice that $\frac{I_{cc}}{\sqrt{U_{cc}^2 - D_{cc}^2}} \sim \frac{I_{cc}}{U_{cc}} \left(1 + \frac{D_{cc}^2}{2U_{cc}^2}\right)$. Therefore, measurements of I_{cc} and U_{cc} determine $\sin[2(\alpha + \theta_d + \delta_\alpha)]$, up to an error that is of second order in D_{cc} (second order in r_0).

and similarly for the complex conjugated channels. After these substitutions and some straightforward algebra we can write a bound similar to that in Eq. (36) as

$$\cos(2\delta_{\pi\pi}) \geq \frac{1}{\sqrt{1-a_{\text{dir}}^2}} \left[1 - 2 \frac{\left(\sqrt{\mathcal{B}(B^0 \rightarrow \pi^0\pi^0)} + \sqrt{\mathcal{B}(\overline{B}^0 \rightarrow \pi^0\pi^0)} \right)^2}{\mathcal{B}(B^0 \rightarrow \pi^+\pi^-) + \mathcal{B}(\overline{B}^0 \rightarrow \pi^+\pi^-)} \right], \quad (38)$$

where

$$a_{\text{dir}} = \frac{\mathcal{B}(B^0 \rightarrow \pi^+\pi^-) - \mathcal{B}(\overline{B}^0 \rightarrow \pi^+\pi^-)}{\mathcal{B}(B^0 \rightarrow \pi^+\pi^-) + \mathcal{B}(\overline{B}^0 \rightarrow \pi^+\pi^-)}. \quad (39)$$

If there is only data on untagged $B \rightarrow \pi^0\pi^0$ decays, we may still obtain a bound by substituting the squared quantity on the right hand side (RHS) of Eq. (38) by $2\mathcal{B}(B^0 \rightarrow \pi^0\pi^0) + 2\mathcal{B}(\overline{B}^0 \rightarrow \pi^0\pi^0)$, a bound previously derived by Charles [8]. If, in addition, there is no data on a_{dir} , then we may obtain a weaker bound by setting a_{dir} to one on the RHS of Eq. (38) [7–9]. In this form, the bound depends only on untagged data and it is related to a bound obtained earlier by Grossman and Quinn [7] by using $B^\pm \rightarrow \pi^+\pi^0$ decays instead of $B \rightarrow \pi^+\pi^-$ decays on the RHS of Eq. (38).

B. A bound from interference effects

One may find a much cleaner bound by rewriting Eq. (33) in the form

$$2\delta_\alpha = \arg \frac{1+x}{1-x}, \quad (40)$$

where

$$x = \frac{r_0}{1-z} = -\frac{D_{cc} + D_{cn}^R + iD_{cn}^I}{U_{cc} + U_{cn}^R + iU_{cn}^I}. \quad (41)$$

We find

$$\tan(2\delta_\alpha) = \frac{2\text{Im}x}{1-|x|^2}. \quad (42)$$

If the quantities z and r_0 are of order one, then we expect to be able to measure them. The case of interest here is when $z \ll 1$, $r_0 \ll 1$, and the best we can do is place bounds on quantities linear in these variables, while we expect to be able to measure U_{cc} and I_{cc} . In this case, we can constrain the allowed values for $\tan(2\delta_\alpha)$ by combining the measurement of U_{cc} with the bounds on U_{cn}^R , U_{cn}^I , D_{cn}^R and D_{cn}^I . (In effect, to gain any information, we need the bounds on the magnitudes of the latter quantities to be smaller than the value for U_{cc} .)

Notice that Eq. (41) involves U_{cn}^R , U_{cn}^I , D_{cn}^R and D_{cn}^I which are linear in a_n and \bar{a}_n . That means that here one is using the interference between the tails of two different $\rho\pi$ channels. This has two consequences. Firstly, this bound, which is extremely powerful, has no analogue for the $B \rightarrow \pi\pi$ decays. Secondly, since the bound depends on the interference effects, it may be sensitive to the assumptions mentioned above about the exact shape of the ρ -resonances.

V. SOME EXPERIMENTAL ISSUES

This analysis has taken a purely formal approach and has not evaluated all the relevant experimental questions. The quantities which we call “mathematically redundant” are actually additional data samples that contribute to fixing the parameters. The parameters we define are all intrinsic to the physical process and hence are, like branching fractions, expected to be the same in any experiment. One issue that will be important experimentally is that the errors on the various parameters are highly correlated and must be treated correctly in establishing bounds such as those from Eq. (42) and the allowed range for α . Moreover, backgrounds, efficiencies, and cuts will differ in the different data samples and must be investigated separately in each case. A good knowledge of the variations in efficiencies across the Dalitz plot is also essential for this analysis. The extraction of the parameter T is sensitive to the knowledge of overall efficiencies; it may be better to simply define a T_{eff} measured separately for each data sample than to depend on the

accuracy with which the overall efficiency and luminosity for each data sample is known. Other caveats have been mentioned, such as the need to explore the sensitivity of the results to reasonable changes in the assumed ρ -shape parameterization, and the recognition of the possible large backgrounds in the untagged sample. All of these issues and many more will only be settled by examining the data.⁶ None of them appear to us to invalidate the expectation that it will be very valuable, at least in the early years of study of these modes, to use the parameters determined from the time-integrated experiments when studying the CP violating effects in the time-dependent data.

VI. CONCLUSIONS

The $B \rightarrow \rho\pi$ decays are described by ten parameters, *c.f.* Eqs. (8) and (9). We have shown that untagged data can be used to extract eight of these ten parameters and tagged time-integrated data allows evaluation of one further parameter. This leaves only the one CP -violating parameter α ($\alpha + \theta_d$ if new physics contributes an extra phase θ_d to the mixing) to be determined from time-dependent data. The parameters in question are defined in an experiment-independent fashion and hence the values measured in a time-integrating experiment, such as can be pursued at CLEO, can be used as input to fits of the time-dependent data sample – thereby possibly allowing a measurement of the parameter $\alpha + \theta_d$ earlier than could be achieved without this input.

We have also shown that, if the neutral ρ contributions are small, then, prior to the time when the statistics are sufficient to provide a measurement of these effects, bounds on their contribution will allow bounds on the shift of the angle measured from the rates and interference of the two charged ρ channels from the true value α .

ACKNOWLEDGMENTS

We are indebted to Y. Gao for discussions concerning the $B \rightarrow \rho\pi$ measurements at CLEO, and to Y. Grossman for discussions regarding the bounds on δ_α and for reading this manuscript. This work is supported by the Department of Energy under contract DE-AC03-76SF00515. The work of J. P. S. is supported in part by Fulbright, Instituto Camões, and by the Portuguese FCT, under grant PRAXIS XXI/BPD/20129/99 and contract CERN/S/FIS/1214/98.

APPENDIX: PARAMETRIZING THE DECAY AMPLITUDES

In this appendix we parametrize the $B^0 \rightarrow \pi^+\pi^-\pi^0$ decay amplitudes by breaking them into CP -even and CP -odd components. This will allow us to see more clearly what quantities may be measured with the various types of experiments. We may decompose the isospin amplitudes into tree-level and penguin contributions as

$$\begin{aligned} A_{3/2,2} &= -T_{3/2,2}e^{i\gamma}, \\ A_{3/2,1} &= -T_{3/2,1}e^{i\gamma}, \\ A_{1/2,1} &= -T_{1/2,1}e^{i\gamma} + P_{1/2,1}e^{-i\beta}, \\ A_{1/2,0} &= -T_{1/2,0}e^{i\gamma} + P_{1/2,0}e^{-i\beta}, \end{aligned} \tag{A1}$$

where we have used the fact that $A_{3/2,1}$ and $A_{3/2,2}$ only receive contributions from the tree-level diagrams. For convenience, we have included an explicit minus sign in the definitions of the tree-level amplitudes. Substituting into Eqs. (1) and (7), and dropping the $\Delta I = 5/2$ amplitude, we find

$$\begin{aligned} e^{i\beta}a_c &= Te^{-i\alpha} \left[\frac{1}{3} + \sqrt{\frac{2}{3}} \frac{T_{1/2,0}}{T} + \sqrt{\frac{2}{3}} \frac{P_{1/2,0}}{T} \cos \alpha + i\sqrt{\frac{2}{3}} \frac{P_{1/2,0}}{T} \sin \alpha \right], \\ e^{i\beta}a_d &= Te^{-i\alpha} \left[\frac{T_{3/2,1}}{T} + \frac{T_{1/2,1}}{T} + \frac{P_{1/2,1}}{T} \cos \alpha + i\frac{P_{1/2,1}}{T} \sin \alpha \right], \\ e^{i\beta}a_n &= Te^{-i\alpha} \left[\frac{2}{3} - \sqrt{\frac{2}{3}} \frac{T_{1/2,0}}{T} - \sqrt{\frac{2}{3}} \frac{P_{1/2,0}}{T} \cos \alpha - i\sqrt{\frac{2}{3}} \frac{P_{1/2,0}}{T} \sin \alpha, \right] \end{aligned} \tag{A2}$$

⁶One can get some idea of the impact of some of them by simulations based on model values for the parameters. Such studies are in progress [16].

where we have defined $T = \sqrt{3}T_{3/2,2}$.

Let us define

$$\begin{aligned}
z &= \frac{2}{3} - \sqrt{\frac{2}{3}} \frac{T_{1/2,0}}{T} - \sqrt{\frac{2}{3}} \frac{P_{1/2,0}}{T} \cos \alpha, \\
z_1 &= \frac{T_{3/2,1}}{T} + \frac{T_{1/2,1}}{T} + \frac{P_{1/2,1}}{T} \cos \alpha, \\
r_0 &= -i \sqrt{\frac{2}{3}} \frac{P_{1/2,0}}{T} \sin \alpha, \\
r_1 &= i \frac{P_{1/2,1}}{T} \sin \alpha.
\end{aligned} \tag{A3}$$

The parameter z_1 (z) contain the CP -even contributions to the final state with isospin $I_f = 1$ ($I_f = 0$ and also $I_f = 2$), while r_1 (r_0) contains the CP -odd penguin contributions to the final state with isospin $I_f = 1$ ($I_f = 0$). Using these definitions, we arrive at

$$\begin{aligned}
e^{i\beta} a_c &= T e^{-i\alpha} (1 - z - r_0), \\
e^{i\beta} a_d &= T e^{-i\alpha} (z_1 + r_1), \\
e^{i\beta} a_n &= T e^{-i\alpha} (z + r_0).
\end{aligned} \tag{A4}$$

Eqs. (8) are obtained from these by dropping the (irrelevant) overall phase factor $e^{i\beta}$. Similarly, we may reach Eqs. (9) by applying CP -conjugation, multiplying by q/p , and removing the same overall phase factor $e^{i\beta}$.

We may also parametrize the amplitudes involved in the $B^\pm \rightarrow \rho^0 \pi^\pm \rightarrow \pi^+ \pi^- \pi^\pm$ and $B^\pm \rightarrow \rho^\pm \pi^0 \rightarrow \pi^\pm \pi^0 \pi^0$ decay chains as

$$e^{\pm i\beta} A_{B^\pm \rightarrow \rho^0 \pi^\pm} = \frac{T e^{\mp i\alpha}}{\sqrt{2}} \left(\frac{1}{2} - z_1 - \delta_1 \mp r_1 \right), \tag{A5}$$

and

$$e^{\pm i\beta} A_{B^\pm \rightarrow \rho^\pm \pi^0} = \frac{T e^{\mp i\alpha}}{\sqrt{2}} \left(\frac{1}{2} + z_1 + \delta_1 \pm r_1 \right), \tag{A6}$$

respectively, where we have dropped the $\Delta I = 5/2$ amplitudes. These decays involve the new complex parameter

$$\delta_1 = -\frac{3}{2} \frac{T_{3/2,1}}{T}. \tag{A7}$$

Therefore, the information in $B^\pm \rightarrow \rho^0 \pi^\pm \rightarrow \pi^+ \pi^- \pi^\pm$ decays by itself does not help in constraining the parameters involved in the decays of the neutral B 's into three pions; these two rates merely allow a determination of the magnitude and phase of δ_1 . The decays from charged B mesons are only useful if one can measure both the $B^\pm \rightarrow \rho^0 \pi^\pm \rightarrow \pi^+ \pi^- \pi^\pm$ and the experimentally challenging $B^\pm \rightarrow \rho^\pm \pi^0 \rightarrow \pi^\pm \pi^0 \pi^0$ decay chains. For example, one might use the information from the decays of the neutral B to get T , r_1 , and z_1 , and the $B^\pm \rightarrow \rho^0 \pi^\pm$ decays to get δ_1 . One would then be able to predict the rates for the $B^\pm \rightarrow \rho^\pm \pi^0$ decays. Even with the additional direct CP asymmetry measurements in these channels, we see that we have no way of extracting a measurement of $\sin \alpha$. As before, only the quantity r_1 appears.

- [1] CDF Collaboration, T. Affolder *et al.*, Fermilab Report Number FERMILAB-PUB-99-225-E (1999), hep-ex/9909003, submitted to Phys. Rev. D.
- [2] M. Gronau and D. London, Phys. Rev. Lett. **65**, 3381 (1990).
- [3] A. E. Snyder and H. R. Quinn, Phys. Rev. D **48**, 2139 (1993).
- [4] CLEO Collaboration, D. Cronin-Hennessy *et al.*, CLEO Report Number CLNS 99/1650, CLEO 99-18 (2000), hep-ex/0001010, unpublished.
- [5] CLEO Collaboration, M. Bishai *et al.*, CLEO Conference Report Number CONF 99-13 (1999), unpublished.

- [6] BABAR Collaboration, *The BaBar physics book*, edited by P. F. Harrison and H. R. Quinn (SLAC, Stanford, 1998). The estimate is that 1200 tagged events will be needed for a good analysis. Using the estimate that 600 untagged events will be collected for 30 fb^{-1} , and a tagging efficiency of $1/3$, this translates into six years at design luminosity.
- [7] Y. Grossman and H. R. Quinn, Phys. Rev. D **58**, 017504 (1998).
- [8] J. Charles, Phys. Rev. D **59**, 054007 (1999).
- [9] D. Pirjol, Phys. Rev. D **60**, 054020 (1999).
- [10] S. Versillé, *La violation de CP dans BaBar: étiquetage des mésons B et étude du canal $B \rightarrow 3\pi$* (Université de Paris Sud, 1999), PhD Thesis.
- [11] R. N. Cahn, J. Charles, F. Le Diberder, and S. Versillé, BaBar Note No. 430.
- [12] H. R. Quinn, review of B physics in C. Caso *et al.*, European Physical Journal **C3**, 1 (1998), and also the URL: <http://pdg.lbl.gov>. See also Y. Grossman and H. R. Quinn, Phys. Rev. D **56**, 7259 (1997).
- [13] J. F. Donoghue, E. Golowich, and B. R. Holstein, *Dynamics of the Standard Model* (Cambridge University Press, Cambridge, 1992).
- [14] G. C. Branco, L. Lavoura, and J. P. Silva, *CP Violation* (Oxford University Press, Oxford, 1999).
- [15] V. Cirigliano, J. F. Donoghue, and E. Golowich, hep-ph/9907341; *ibid* hep-ph/9909473.
- [16] R. N. Cahn, private communication.

Observable	Coefficient of $\sin 2(\alpha + \theta_d)$	Coefficient of $\cos 2(\alpha + \theta_d)$
I_{cc}	$ 1 - z ^2 - r_0 ^2$	$2\text{Im}[r_0(1 - z)^*]$
I_{dd}	$ r_1 ^2 - z_1 ^2$	$2\text{Im}[r_1 z_1^*]$
I_{cd}^I	$2\text{Re}[r_1(1 - z)^* + z_1 r_0^*]$	$2\text{Im}[(1 - z)z_1^* + r_0 r_1^*]$
I_{cd}^R	$2\text{Im}[r_1(1 - z)^* + z_1 r_0^*]$	$2\text{Re}[(1 - z)z_1^* + r_0 r_1^*]$
I_{cn}^I	$2\text{Re}[z - z ^2 + r_0 ^2]$	$2\text{Im}[(1 - 2z)r_0^*]$
I_{cn}^R	$2\text{Im} z$	$2\text{Re} r_0$
I_{dn}^I	$2\text{Re}[z r_1^* - r_0 z_1^*]$	$2\text{Im}[r_1 r_0^* - z_1 z^*]$
I_{dn}^R	$2\text{Im}[z r_1^* - r_0 z_1^*]$	$2\text{Re}[r_1 r_0^* - z_1 z^*]$
I_{nn}	$ z ^2 - r_0 ^2$	$2\text{Im}[z r_0^*]$

TABLE I. I -observables obtained from the $\sin \Delta m t$ term. The table shows their dependence on $\sin 2(\alpha + \theta_d)$ and $\cos 2(\alpha + \theta_d)$.